J. Plasma Fusion Res. SERIES, Vol. 5 (2002) 570–573

Numerical Analysis on the He II Heat Transport in Channels with a Porous Spacer

HAMAGUCHI Shinji, YANAGI Nagato, SATOW Takashi and OKAMURA Tetsuji[1]

National Institute for Fusion Science, Toki 509-5292, Japan

[1] Tokyo Institute of Technology, Yokohama 226-8502, Japan

(Received: 11 December 2001 / Accepted: 6 August 2002)

Abstract

Heat transport characteristics in a pressurized He II channel have been studied, using two-dimensional numerical code that is based on the two fluid model. In general, He II heat transport performance gets worse in a either long or narrow channel [1]. If a porous medium is used as a part of the channel to transfer heat to a next channel, it will be expected to improve the heat transport in the channel. In this study, numerical model was based on the channel formed by two FRP plates in parallel and a spacer was inserted in the middle of the channel to divide into two regions. A heater was placed in one of FRP plate to input heat to the channel. Two kinds of spacers were used in the analysis to compare heat transport characteristics; (1) porous spacer, (2) FRP spacer. The temperature distribution and flow velocity vectors of He II in the channel were calculated with a steady state heat input. According to the calculated results, the temperature increase of He II in the heated channel was suppressed in the case of a porous spacer. In addition, the mass flow induced by the thermo-mechanical effect of He II enhanced heat transport capability. The paper also discusses the He II flows within the channel.

Keywords:

He II, heat transport, porous spacer, numerical analysis, two fluid model, thermo-mechanical effect

1. Introduction

Since the cooling channels of superconducting magnets are narrow and complicated, it is important to investigate the heat transport characteristics of He II in the channels. To use the pressurized He II for the coolant of LHD's helical coils, R&D are being conducted for heat transport characteristics of He II channels at the National Institute for Fusion Science [2].

In the present research, a numerical code, which is named SUPER-2D, developed by Rao *et al.* and extended by Tatsumoto *et al.* was used [3-5]. The code is based on the two fluid model and can solve problems of two-dimensional heat transport in He II channels. So far, most analysis using this code had been carried out on static He II. In the present studies, dynamic heat transport problems will be analyzed in a channel tested by Okamura *et al.* [6]. The channel was separated into two regions by a porous spacer. When heat was applied to one region of the channel, helium flowed through the spacer. The numerical code is applied to the channel where the complex He II flows exist.

2. Numerical Analysis

2.1 Experimental Model

Okamura *et al.* had carried out experiments on heat transport of a He II channel in which a spacer was inserted. According to their experiments, the use of a porous spacer in the middle of a He II channel could reduce the temperature increase in the heated region. It

Corresponding author's e-mail: hamaguchi@LHD.nifs.ac.jp

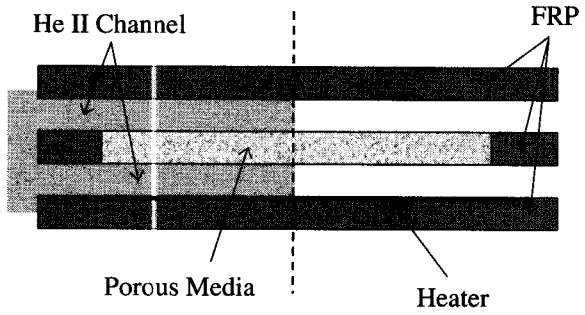

Fig. 1 A schematic of the channel used in the present analysis.

implied that He II flows were induced through a porous medium by the thermo-mechanical effect. However, the He II flows were not measured because it was difficult to measure the flow velocities in the whole channel. In the present analysis, not only helium temperature changes but also the He II flows were calculated in the channel.

A schematic of the channel, formed in glass fiber reinforced plastic plates, for the analysis is shown in Fig. 1. The channel is 170 mm long and 7 mm wide. A spacer 5 mm thick is used to separate two rectangular channels of the same shape, which is inserted in the middle of a channel to divide into two regions. Each region is 3 mm high. Two kinds of spacers are used in the present analysis to compare heat transport characteristics; (1) porous spacer, (2) FRP spacer. The porous spacer is replaced by a porous medium at the center portion of the FRP spacer. The length of the porous medium is 150 mm and the porosity is 22 %. A heater, 170 mm long, is attached at bottom the channels. Both ends of the channel are kept open to a He II bath at atmospheric pressure. The channels are placed horizontally in the He II bath.

2.2 Numerical Model

A set of the following basic equations is used in the analysis.

Equation of continuity;

$$\frac{\partial}{\partial t}\left(\rho_s+\rho_n\right)+\nabla\cdot\left(\rho_s \boldsymbol{u}_s+\rho_n \boldsymbol{u}_n\right)=0.$$

Equation of motion for total fluid of He II;

$$\frac{\partial}{\partial t}\left(\rho_s \boldsymbol{u}_s+\rho_n \boldsymbol{u}_n\right)$$
$$=-\nabla\cdot\left(\rho_s \boldsymbol{u}_s \boldsymbol{u}_s+\rho_n \boldsymbol{u}_n \boldsymbol{u}_n\right)-\nabla P$$
$$+\eta\left(\nabla^2 \boldsymbol{u}_n+\frac{1}{3}\nabla\left(\nabla\cdot \boldsymbol{u}_n\right)\right)+\rho \boldsymbol{g}.$$

Equation of motion for superfluid component;

$$\frac{\partial \boldsymbol{u}_s}{\partial t}=-\left(\boldsymbol{u}_s\cdot\nabla\right)\boldsymbol{u}_s+s\nabla T$$
$$-\frac{1}{\rho}\nabla P+\frac{\rho_n}{2\rho}\nabla\left|\boldsymbol{u}_n-\boldsymbol{u}_s\right|^2$$
$$+A_{GM}\rho_n\left|\boldsymbol{u}_n-\boldsymbol{u}_s\right|^2\left(\boldsymbol{u}_n-\boldsymbol{u}_s\right)+\boldsymbol{g}.$$

Equation of entropy;

$$\frac{\partial}{\partial t}(\rho s)=-\nabla\cdot(\rho s \boldsymbol{u}_n)$$
$$+\frac{\eta}{T}\left\{\frac{\partial u_{ni}}{\partial x_j}\frac{\partial u_{ni}}{\partial x_j}+\frac{\partial u_{nj}}{\partial x_i}\frac{\partial u_{ni}}{\partial x_j}-\frac{2}{3}\left(\nabla\cdot \boldsymbol{u}_n\right)^2\right\}$$
$$+\frac{A_{GM}\rho_n\left|\boldsymbol{u}_n-\boldsymbol{u}_s\right|^4}{T}.$$

The above equations are solved, using the numerical code named SUPER-2D. As shown in Fig. 1, the left half of the channel is analyzed because of a symmetric problem. The analytical area is divided into 340×24 rectangular mesh with the length of 0.25 mm. Time step is set to be 4×10^{-7} s and time integration is carried out explicitly. The adiabatic condition is used at the FRP surfaces, where velocities of the total fluid and normal component are zero. The slip condition is applied to velocities of the superfluid component at the surfaces. The heat is applied uniformly to the heater surface and the value of heat flux is kept at 0.1 W/cm^2. The temperature of the ends of channels is kept at the He II bath temperature of 1.92 K. It is defined that only the superfluid component can flow in the vertical direction through the porous medium and the non-slip condition is applied to the normal fluid component on surfaces of the porous medium.

3. Numerical Results

3.1 Temperature Distribution

The temperature distributions just before the lambda transition in the channel are shown in Figs. 2(a) and (b), which represent the numerical results in the case of the porous spacer and the FRP spacer, respectively. The left side of the figures is the channel end, while the right side is the center of the channel. The heater is placed at the bottom. The black rectangles in the middle of the channel show the spacer. An interval of isothermal lines is 0.02 K.

In the case of the porous spacer, it took 175 ms to reach the lambda transition of He II at the center of the heater surface. As the heat was applied to the lower region of the channel, the temperature of the lower

region as well as the upper region increased. The heat would be carried away, using the two regions of the channel. The maximum of temperature difference between two regions were 0.01 K at the center of channel.

In the case of the FRP spacer, the temperature in the upper region kept at the initial temperature because the heat could not transfer from the lower region to the upper region owing to the FRP spacer. The heat transport was limited to only the lower region, so the temperature in the channel increased quickly. It took 66 ms to reach the lambda transition. The maximum of temperature difference between two regions were 0.24 K at the center of channel.

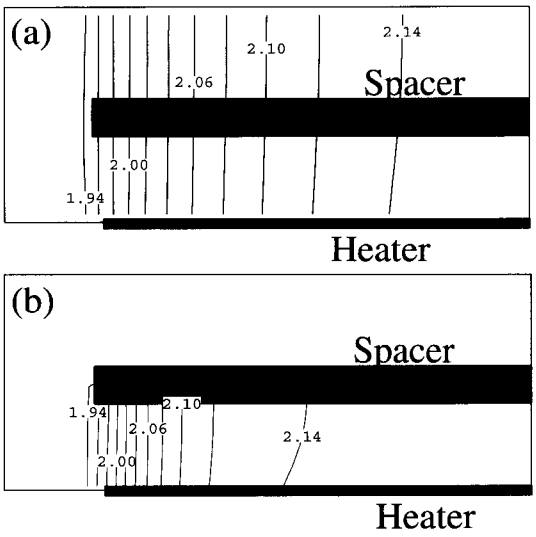

Fig. 2 Temperature distributions of the channel.
(a) porous spacer, (b) FRP spacer.

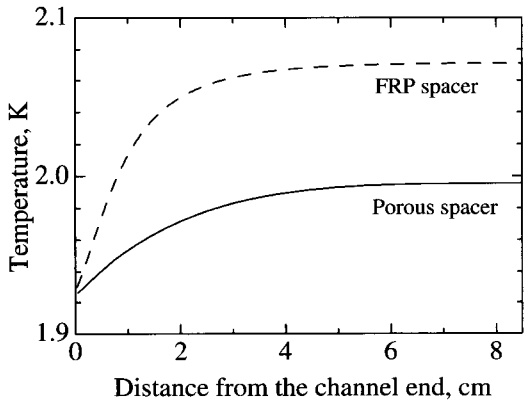

Fig. 3 Temperature distribution of the heated region.

To compare the heat transport characteristics of the two channels under the same initial conditions, the temperature distributions at the middle of the heated regions are shown in Fig. 3. Solid and dashed lines represent the numerical results in the case of the channel with the porous spacer and with the FRP spacer, respectively. The computational time was 40 ms. In the case of the porous spacer, the temperature of heated region kept lower than in the case of the FRP spacer. The heat transport characteristics were improved in the channel where the porous spacer was inserted.

3.2 Induced Flows of He II through Porous Spacer

Figure 4 shows the flow velocities of the total fluid, normal fluid component and superfluid component in the channel including the porous spacer. The black rectangles in the middle of the channel display the porous spacer. Each vector in the figure expresses both magnitude and direction of flow velocity at each point. Concerning the total fluid, He II went into the channel from the open bath, and passed by the porous spacer, flowed out from the channel. These flows were induced by temperature differences between two regions, that is, the thermo-mechanical effect. The He II flows promoted the heat transport in the channel.

In the case of the superfluid component, it entered in the channel from the bath, flowed through the porous spacer and streamed toward the heater at last. On the other hand, the normal fluid component was generated

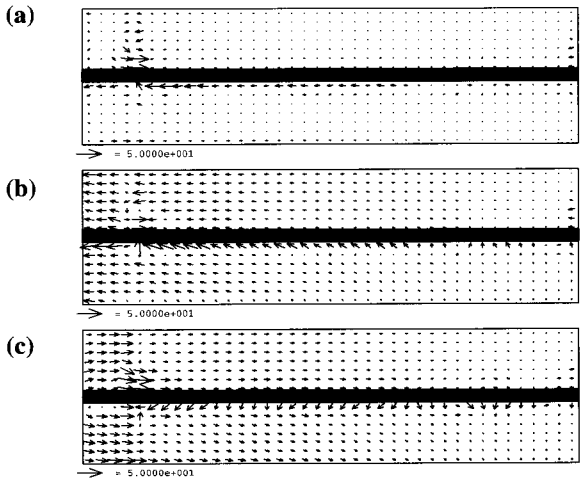

Fig. 4 Flow velocity vectors in the channel with the porous spacer.
(a) total fluid, (b) normal fluid, (c) superfluid.

on the heater surface and then went away, spreading over the whole channel. Therefore, the superfluid component flowed with the total flow in the upper region, while it flowed against the total flow in the lower region. In the case of the normal fluid, the counter flow was generated against the flows of the superfluid component.

3.3 Comparison with Experimental Results

Figure 5 shows the temperature distribution in the channel with the porous spacer. Solid line and circles represent the numerical and experimental results, respectively. A similar tendency of the temperature distribution was obtained but there were the 30 % discrepancy between the experiments and the analysis. That would be because the numerical code could not deal with a large pressure drop across the porous medium and therefore the present numerical model was modified to make the pressure changes small on both surfaces of the porous medium. So the flow velocity of the analysis would be underestimated, compared with the experiments.

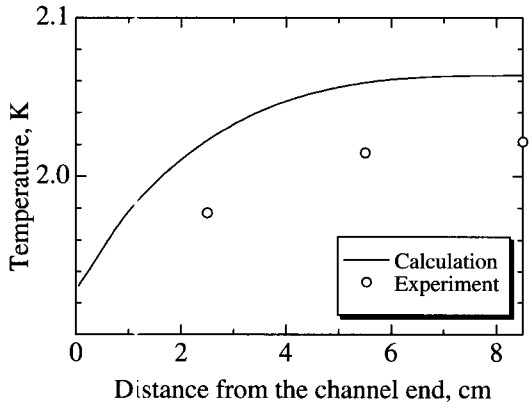

Fig. 5 Temperature distribution in the channel.

4. Conclusions

The heat transfer characteristics of He II channels, divided into two regions by a spacer, have been numerically investigated by using the numerical code based on the two fluid model. The temperature and the velocities distributions of total fluid, normal fluid component and superfluid component were analyzed in the channel. As a result, the He II flows induced by the thermo-mechanical effect were obtained. Even though, the temperature profiles were similar, the discrepancies are relatively large. It implied that the flows had significant effects on the heat transport of the channel in the experiments.

Acknowledgement

The authors would like to thank Prof. M. Shiotsu, Mr. H. Tatsumoto and Prof. K. Fukuda for their helpful suggestions. The authors also appreciate Dr. R. Maekawa to review the paper. The present work was partially supported by the Ministry of Education, Science, Sports and Culture of Japan, Grant-in-Aid for Science Research (A), 2000.

References

[1] S.W. Van Sciver, *Helium Cryogenics* (Plenum Press, New York (1986)).
[2] J. Yamamoto *et al.*, ICEC16/ICMC Proceedings, 731 (1996).
[3] Y.F. Rao *et al.*, Cryogenics **36**, 457 (1996).
[4] H. Tatsumoto *et al.*, Cryogenics **42**, 9 (2002).
[5] H. Tatsumoto *et al.*, Cryogenics **42**, 19 (2002).
[6] T. Okamura *et al.*, Cryogenics **38**, 967(1998).